



# SYNTHESIS AND SORPTION STUDIES OF THE DEGRADATION OF CONGO RED BY Ni-Fe LAYERED DOUBLE HYDROXIDE

N. AYAWEI<sup>a,\*</sup>, J. GODWIN<sup>a</sup> and D. WANKASI<sup>a,b</sup>

<sup>a</sup>Department of Chemical Sciences, Niger Delta University, Wilberforce Island,  
BAYELSA STATE, NIGERIA

<sup>b</sup>Applied Chemistry and Nanoscience Laboratory, Department of Chemistry,  
Vaal University of Technology, P. O. Box X021, VANDERBIJLPARK, SOUTH AFRICA

## ABSTRACT

Layered double hydroxide (Ni/Fe-CO<sub>3</sub>) was synthesized by co-precipitation method and characterized by X-ray diffraction (XRD), Fourier Transform Infrared spectroscopic (FTIR) and energy-dispersive X-ray spectroscopic (EDX) and applied for degradation of Congo red dye. The batch adsorption experiments were carried out to study the effect of various parameters, such as (CR) the initial concentration, contact time and temperature on adsorption properties of congo red onto the layered double hydroxide. The applicability of Langmuir, Freundlich, Dubinin-kaganer-Radushkevich and Temkin adsorption isotherm equations for the present system was also tested. The experimental data fitted all studied isotherm models with correlation coefficient values of 0.9995, 0.9973, 0.9982 and 0.9992, respectively. The kinetic studies showed that the adsorption data followed the pseudo-second order model. Thermodynamic studies indicated the adsorption of Congo red onto the layered double hydroxide was a spontaneous and endothermic process.

**Key words:** Layered double hydroxides, Kinetic, Dye, Adsorption, Isotherms, Congo red, Thermodynamics.

## INTRODUCTION

Approximately 10% of total dye production per year is not used but discharged into water bodies. This has placed premium on scientists and governments all over the world to look at the impacts of such discharges. A large variety of dyestuffs is available under the categories of acid, basic, reactive, direct, disperse, sulphur and metallic dyes<sup>1</sup>. Dyes are synthetic aromatic compounds, which have various functional groups<sup>2</sup>. Some dyes and their degradation products may be carcinogens and toxic, and consequently their treatment cannot

---

\* Author for correspondence; E-mail: [ayawei4acad@gmail.com](mailto:ayawei4acad@gmail.com)

depend on biodegradation alone<sup>3,4</sup>. Therefore, extensive research has been conducted to find an effective and efficient alternative for the removal of dyes. The adsorption process is one of the effective methods for removal dyes from the waste sewage<sup>5,6</sup>. The process of adsorption has an advantage over the other methods due to its sludge free clean operation and completely removed dyes, even from the diluted solution.

Layered double hydroxide (LDH) is a class of anionic clays with high anion exchange capacities, which can be used as an effective adsorbent for the removal of variety of anionic pollutant. Their empirical formula of LDH can be described by the formula  $[M^{2+}_{1-x}M^{3+}_x(OH)_2]^{x+}(A^{n-})_{x/n}.mH_2O$ , where  $M^{2+}$  and  $M^{3+}$  are metal cations, for example  $Mg^{2+}$  and  $Al^{3+}$ , respectively, that occupy octahedral sites in the hydroxide layers,  $A^{n-}$  is an exchangeable anion and  $x$  is the ratio  $M^{3+}/(M^{2+} + M^{3+})$ . Carbonates are the interlayer anions in the naturally occurring mineral hydroxides, which is a member of this class of materials<sup>7,8</sup>. It is known that many substances in waste water, such as humic acid substances, dye in the effluents carry negative charges<sup>9</sup>. Species that carry negative charges account for a large part of water in the water systems<sup>10</sup>. Because of the large surface area, anion exchange ability, and regeneration ability, LDHs are used as adsorbents for purification of wastewater<sup>11,12</sup>. This work aims to replicate clay like materials in a laboratory condition, optimize process conditions for the removal of dyes in aqueous solutions.

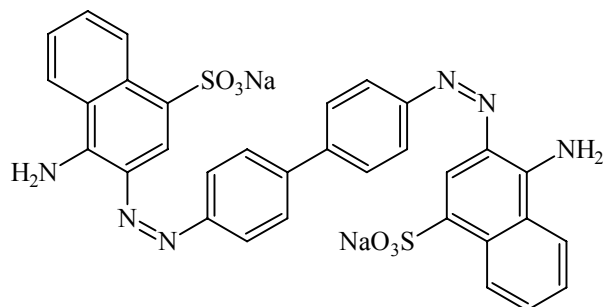


**Fig. 1: Molecular formula of congo red**

## EXPERIMENTAL

### Materials and methods

#### Synthesis of LDH

Carbonate form of Ni-Fe LDH was synthesized by co-precipitation method. A 50 mL aqueous solution containing 0.3 M  $Ni(NO_3)_2 \cdot 6H_2O$  and 0.1 M  $Fe(NO_3)_3 \cdot 9H_2O$  with Ni/Fe ratios 3:1, was added drop wise into a 50 mL mixed solution of  $(NaOH (2M) + Na_2CO_3$

(1 M) with vigorous stirring and maintaining a pH of greater than 10 at room temperature. After complete addition, which last between 2 hrs 30 mins to 3 hrs, the slurry formed was aged at 60°C for 18 hrs. The products were centrifuged at 5000 rpm for 5 mins, with distilled water 3-4 times and dried by freeze drying.

### **Preparation of congo red solution**

Congo red (CI = 22120) was supplied by Merck (Mumbai, India). A stock solution of CR dye was prepared (100 mg/L) by dissolving a required amount of dye powder in deionized water. The stock solution was diluted with deionized water to obtain the desired concentration ranging from 20 to 100 mg/L.

The concentration of CR in the experimental solution was determined from the calibration curve prepared by measuring the absorbance of different known concentrations of CR solutions at  $\lambda_{\text{max}} = 497$  nm using a UV-vis spectrophotometer (Shimadzu, Kyoto, Japan). The pH meter using a combined glass electrode (Model HI 9025C, Hanna instruments, Singapore).

### **Characterization of layered double hydroxide**

A Shimadzu XRD 6000 Diffractometer with nickel filtered Cu-K $\alpha$  ( $\lambda = 0.1542$  nm) beam operated at 30 kV and 30 mA was used to determine the interlayer d-spacing of the clay layer in the original Ni-Fe LDH, modified stearate Ni-Fe LDH, blends and nanocomposites using Bragg's equation  $n\lambda = 2d\sin\theta$ . Data were recorded in  $2\theta$  range of 2°–30° using the scan rate of 2°/min.

The functional groups, types of bonding and identify components in the samples were determined by a Perkin-Elmer Spectrum 1000 series Spectrophotometer equipped with attenuated total reflectance (ATR). The infrared spectra of the samples were recorded in the range of frequency of 400–4,000  $\text{cm}^{-1}$ .

FESEM/EDX was obtained using Carl Zeiss SMT supra 40 VPFESEM Germany and inca penta FET x 3 EDX, Oxford. It was operated at extra high tension (HT) at 5.0 kV and magnification at 20000X. FESEM uses electron to produce images (morphology) of samples and was attached with EDX for qualitative elemental analysis.

### **Experimental procedure**

Batch adsorption experiments were carried out to study the effect of initial congo red concentration, contact time and temperature on the adsorption of congo red on the layered double hydroxide. Adsorption studies were carried out using 25 mL of each dye solution and

0.2 g of the adsorbent. At the end of each experiment, the content of each tube was filtered using a Whatman No 14 filter paper after which the concentration of residual congo red was determined by UV-Vis spectrophotometer analysis. All experiments were carefully conducted to acquire good result.

In order to determine the rate of adsorption, experiments were conducted with different initial concentrations of dyes ranging from 20 to 40 mg/L. All other factors are kept constant. The adsorption experiments were performed at three different temperatures viz., 40, 60 and 80°C in a thermostat attached with a shaker (Remi make). The constancy of the temperature was maintained with an accuracy of  $\pm 0.5^\circ\text{C}$ .

The effect of period of contact on the removal of the dye on adsorbent in a single cycle was determined by time intervals of 10, 20 and 30 mins.

The adsorption capacity and the removal efficiency of congo red by the layered double hydroxide were analyzed using equations 1 and 2, respectively.

$$q_{\text{eq}} = \frac{C_{\text{init}} - C_{\text{eq}}}{m} \quad \dots(1)$$

$$R\% = \frac{C_{\text{init}} - C_{\text{eq}}}{C_{\text{eq}}} \times 100 \quad \dots(2)$$

where  $C_{\text{init}}$  and  $C_{\text{eq}}$  are, respectively, the initial and equilibrium concentrations of metal ions in solution (mmol/L) and  $m$  is the layered double hydroxide dosage (g/L).

### **Isotherms analysis**

The data for the uptake of Congo red at different temperatures has been processed in accordance with the linearised form of the Freundlich and Langmuir isotherm equations.

For the Freundlich isotherm the In-In version was used:

$$\ln q_{\text{eq}} = \ln K_f + \frac{1}{n} \ln C_{\text{eq}} \quad \dots(3)$$

The Langmuir model linearization (a plot of  $1/q_{\text{eq}}$  vs  $1/C_{\text{eq}}$ ) was expected to give a straight line with intercept of  $1/q_{\text{max}}$ :

$$\frac{1}{q_{\text{eq}}} = \frac{1}{K_1 q_{\text{mas}} C_{\text{eq}}} + \frac{1}{q_{\text{eq}}} \quad \dots(4)$$

The essential characteristics of the Langmuir isotherm were expressed in terms of a dimensionless separation factor or equilibrium parameter  $S_f$ .

$$S_f = \frac{1}{1 + aC_o} \quad \dots(5)$$

With  $C_o$  as initial concentration of Congo red in solution, the magnitude of the parameter  $S_f$  provides a measure of the type of adsorption isotherm. If  $S_f > 1.0$ , the isotherm is unfavourable;  $S_f = 1.0$  (linear);  $0 < S_f < 1.0$  (favourable) and  $S_f = 0$  (irreversible).

The DKR isotherm is reported to be more general than the Langmuir and Freundlich isotherms. It helps to determine the apparent energy of adsorption. The characteristic porosity of adsorbent toward the adsorbate and does not assume a homogenous surface or constant sorption potential<sup>13</sup>.

The Dubinin–Kaganer–Radushkevich (DKR) model has the linear form

$$\ln q_e = \ln X_m - \beta \varepsilon^2 \quad \dots(6)$$

where  $X_m$  is the maximum sorption capacity,  $\beta$  is the activity coefficient related to mean sorption energy, and  $\varepsilon$  is the Polanyi potential, which is equal to –

$$\varepsilon = RT \ln \left( 1 + \frac{1}{C_e} \right) \quad \dots(7)$$

where  $R$  is the gas constant (kJ/kmol). The slope of the plot of  $\ln q_e$  versus  $\varepsilon^2$  gives  $\beta$  ( $\text{mol}^2/\text{J}^2$ ) and the intercept yields the sorption capacity,  $X_m$  (mg/g) as shown in Equation 6. The values of  $\beta$  and  $X_m$ , as a function of temperature are listed in Table 1 with their corresponding value of the correlation coefficient,  $R^2$ . It can be observed that the values of  $\beta$  increase as temperature increases while the values of  $X_m$  decrease with increasing temperature.

The values of the adsorption energy,  $E$ , was obtained from the relationship<sup>14</sup>.

$$E = (2\beta)^{-1/2} \quad \dots(8)$$

The Temkins isotherm model was also applied to the experimental data, unlike the Langmuir and Freundlich isotherm models, this isotherm takes into account the interactions between adsorbents and metal ions to be adsorbed and is based on the adsorption that the free energy of adsorption is simply a function of surface coverage<sup>15</sup>. The linear form of the Temkins isotherm model equation is given in Eq. (9).

$$q_e = B \ln A + B \ln C_e \quad \dots(9)$$

Where  $B = [RT/b_T]$  in (J/mol) corresponding to the heat of adsorption,  $R$  is the ideal gas constant,  $T(K)$  is the absolute temperature,  $b_T$  is the Temkins isotherm constant and  $A$  (L/g) is the equilibrium binding constant corresponding to the maximum binding energy.

### Kinetic parameters

The experimental data were further subjected to certain kinetic parameters.

Zero-order kinetic model,

$$q_t = q_0 + K_0 t \quad \dots(10)$$

First-Order Kinetic model,

$$\ln q_t = \ln q_0 + K_1 t \quad \dots(11)$$

Second-Order Kinetic model,

$$\frac{1}{q_t} = \frac{1}{q_0} + K_2 t \quad \dots(12)$$

Third-order kinetic model

$$\frac{1}{q_t^2} = \frac{1}{q_0^2} + K_3 t \quad \dots(13)$$

Pseudo-second order model

$$\frac{t}{q_t} = \frac{1}{h_0} + \frac{1}{q_e} t \quad \dots(14)$$

### Thermodynamic parameters

Thermodynamic parameters such as change in Gibb's free energy  $\Delta G^\circ$ , enthalpy  $\Delta H^\circ$  and entropy  $\Delta S^\circ$  were determined using the following equation:

$$K_d = \frac{q_{eq}}{C_{eq}} \quad \dots(15)$$

where  $K_d$  is the apparent equilibrium constant,  $q_{eq}$  (or  $[Congo\ Red]_{uptake}$ ); is the amount of metal adsorbed on the unitary sorbent mass (mmol/g) at equilibrium and  $C_{eq}$  (or  $[Congo\ Red]_{eq}$ ) equilibrium concentrations of metal ions in solution (mmol/L), when

amount adsorbed is equals  $q_{\text{eq}}$ ;  $-\frac{q_{\text{eq}}}{C_{\text{eq}}}$  relationship depends on the type of the adsorption that occurs, i.e. multi-layer, chemical, physical adsorption, etc.

The thermodynamic equilibrium constants ( $K_d$ ) of the Congo red adsorption on studied layered double hydroxide were calculated by the method from the intercept of the plots of  $\ln(q_{\text{eq}}/C_{\text{eq}})$  vs.  $q_{\text{eq}}$ .

Then, the standard free energy change  $\Delta G^\circ$ , enthalpy change  $\Delta H^\circ$  and entropy change  $\Delta S^\circ$  were calculated from the Van't-Hoff equation.

$$\Delta G^\circ = -RT \ln K_d \quad \dots(16)$$

where  $K_d$  is the apparent equilibrium constant; T is the temperature in Kelvin and R is the gas constant ( $8.314 \text{ Jmol}^{-1}\text{K}^{-1}$ ):

The slope and intercept of the Van't-Hoff plot of  $\ln K_d$  vs.  $1/T$  were used to determine the values of  $\Delta H^\circ$  and  $\Delta S^\circ$ ,

$$\ln K_d = \left[ -\frac{\Delta H^\circ}{R} \right] \frac{1}{T} + \frac{\Delta S^\circ}{R} \quad \dots(17)$$

Then, the influence of the temperature on the system entropy was evaluated using the equations<sup>11</sup>. The plot of  $\Delta G^\circ$  vs.  $t$  also give the result of  $\Delta H^\circ$  and  $\Delta S^\circ$ .

$$\Delta G^\circ = \Delta H^\circ - T\Delta S^\circ \quad \dots(18)$$

The thermodynamic parameters of the adsorption were also calculated by using the Langmuir constant ( $K_L$ ), Freundlich constants ( $K_F$ ) for the equations instead of ( $K_d$ ). The obtained data on thermodynamic parameters were compared, when it was possible.

The differential isosteric heat of adsorption ( $\Delta H_x$ ) at constant surface coverage was calculated using the Clausius-Clapeyron equation:

$$\frac{d \ln(C_{\text{eq}})}{dT} = -\frac{\Delta H_x}{RT^2} \quad \dots(19)$$

Integration gives the following Equation 20.

$$\ln(C_{\text{eq}}) = \frac{\Delta H_x}{R} \frac{1}{T} + k \quad \dots(20)$$

where  $K$  is a constant. The differential isosteric heat of adsorption was calculated from the slope of the plot of  $\ln(C_{\text{eq}})$  vs  $1/T$  and was used for an indication of the adsorbent surface heterogeneity. For this purpose, the equilibrium concentration ( $C_{\text{eq}}$ ) at constant amount of adsorbate adsorbed was obtained from the adsorption isotherm data at different temperatures.

In order to further support the assertion that physical adsorption is the predominant mechanism, the values of activation energy ( $E_a$ ) and sticking probability ( $S^*$ ) were estimated from the experimental data. They were calculated using modified Arrhenius type equation related to surface coverage ( $\theta$ ) as follows:

$$\theta = \left[ 1 - \frac{C_e}{C_i} \right] \text{ or } \frac{C_e}{C_i} = 1 - \theta \quad \dots(21)$$

$$S^* = (1 - \theta) e^{-\frac{E_a}{RT}} \quad \dots(22)$$

$$\ln S^* = \ln(1 - \theta) - \frac{E_a}{RT} \quad \dots(23)$$

$$\ln(1 - \theta) = \ln S^* + \frac{E_a}{RT} \quad \dots(24)$$

## RESULTS AND DISCUSSION

### Characterization of LDH

#### SEM

Figs. 2 shows the pre & post adsorption SEM images. The SEM image of post adsorption shows coverage of available pores in relation to pre-adsorption image.

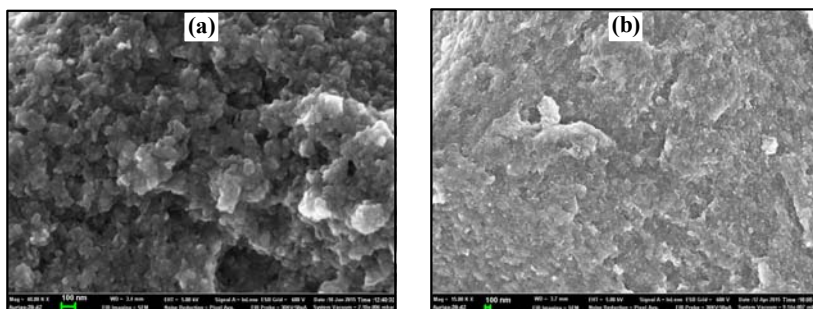


**Fig. 2: Scanning electron microscope (SEM) micrograph of Ni/Fe-CO<sub>3</sub> (a) before and (b) after adsorption studies**

## FT-IR

Fig. 3 shows the pre and post adsorption FT-IR spectra of the Ni/Fe-LHD. The strong bond around  $3400\text{ cm}^{-1}$  is associated with the stretching vibration of OH groups in the brucite like layer and interlayer inter molecules as shown in Fig. 3(a). The broadening of the bond was attributed to the hydrogen-bond formation. Less intense absorption bond around  $1650\text{-}1500\text{ cm}^{-1}$  was assigned to the bending vibration of the interlayer water molecules. The carbonate ion peak is around  $1400\text{ cm}^{-1}$ , which is consistent with layered double hydroxides. The low wave number region of  $< 1000\text{ cm}^{-1}$ , the lattice vibration modes of the layered double hydroxides sheets such as M-O is assigned between  $840\text{-}550\text{ cm}^{-1}$ . New peaks round  $650\text{-}900\text{ cm}^{-1}$  and  $1100\text{-}1200\text{ cm}^{-1}$  are due to wagging bending vibration of primary amines and symmetric and asymmetric stretching of S=O and aromatic ring vibration. The adsorption process thus follows the formation of complex between the congo red and double layered double hydroxide<sup>16</sup>.

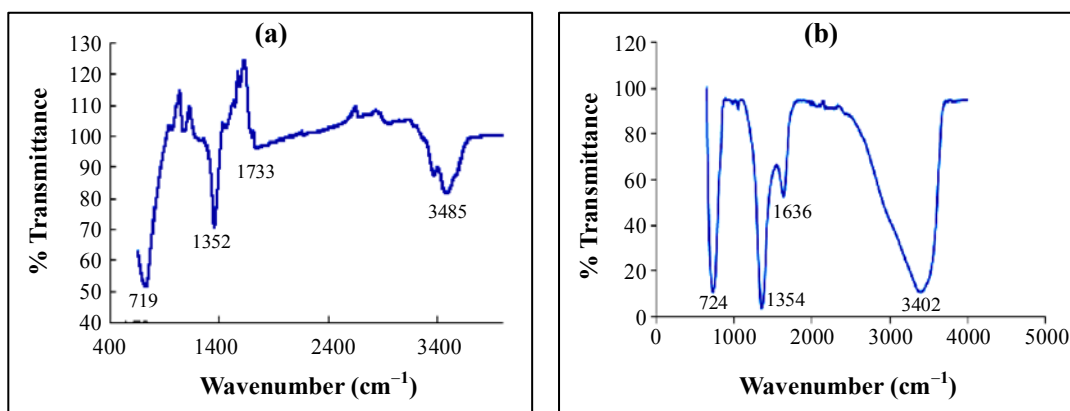


**Fig. 3: Ni/Fe- $\text{CO}_3$  Fourier transform infrared spectroscopy, (a) before and (b) after adsorption studies**

## XRD

Fig. 4 shows the XRD patterns of the Ni/Fe. It exhibits the typical profile for LDH materials with sharp intense peak at low theta values, whereas they become weaker and less defined at higher angular values. No residual peaks were observed thus confirming the absence of contaminant phases. Basal peaks were located near  $2\theta$  of  $8.44\text{ \AA}$ ,  $22.24\text{ \AA}$  and  $34.04\text{ \AA}$  corresponding to diffraction by (003), (006) and (009) planes and d-spacing of 1.04 nm, 0.3992 nm and 0.2631 nm, respectively. These three peaks shows te presence of an ordered layered structure.

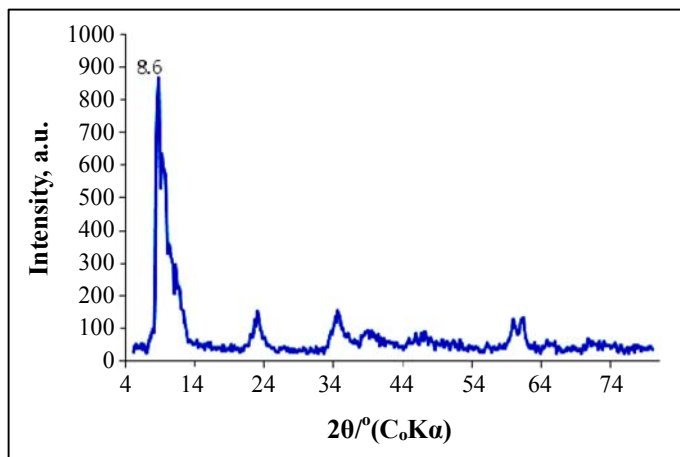


Fig. 4: Ni/Fe-CO<sub>3</sub> X-ray powder diffraction

### Effect of concentration

Removal efficiency of Congo red by adsorbents is illustrated in Fig. 5. It shows that removal efficiency decreased with increasing of initial concentration (54%, 51% and 48.8%), respectively. This is probably due to rapid adsorption at all available site and relatively small amount of adsorbent that was used, an increase in the amount of adsorbent may therefore, reverse adsorption trend.

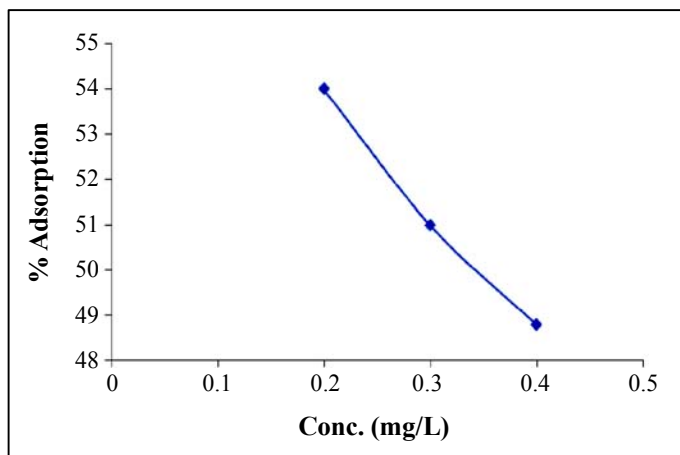
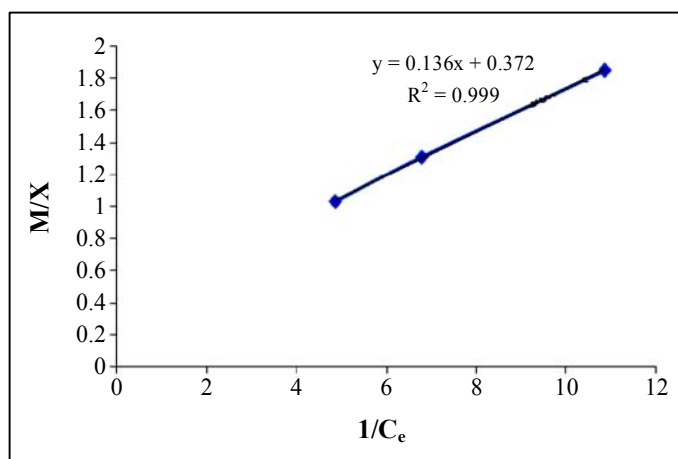


Fig. 5: Effect of concentration on adsorption of Congo red onto layered double hydroxide

### Isotherm analysis

To investigate an interaction of adsorbate molecules and adsorbent surface, four well-known models, the Langmuir, Freundlich, Dubinin-kaganer-radushkevich and Temkin isotherms, were selected to explicate LDH interaction in this study. The Langmuir plot in Fig. 6 fitted the experimental data with  $R^2 = 0.9995$  and therefore, confirm monolayer coverage.

The influence of isotherm shape on whether adsorption is favourable or unfavourable has been considered. For a Langmuir type adsorption process, the isotherm shape can be classified by a dimensionless constant separation factor ( $R_L$ ), given by Eq. (4). The calculated value of  $R_L$  from Fig. 6 is 0.714, which is within the range of 0-1, thus confirms the favourable uptake of the layered double hydroxide adsorption process. The degree of favourability is generally related to the irreversibility of the system, giving a qualitative assessment of the layered double hydroxide interactions. The degrees tended toward zero (the completely ideal irreversible case) rather than unity (which represents a completely reversible case).



**Fig. 6: Langmuir isotherm plot for adsorption of Congo red onto layered double hydroxide**

The adsorption capacity of the layered double hydroxide was extrapolated from the slope of the plot of Freundlich to be 0.939 in Fig. 7. The fraction of the layered double hydroxide surface covered by the Congo red is given as 0.54 (Table 1). This value indicates that 54% of the pore spaces of the Layered double hydroxide surface were covered by the Congo red, which means high degree of adsorption.

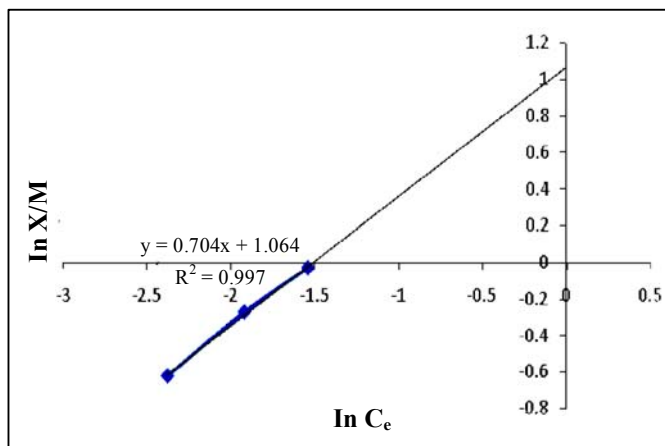


**Fig. 7: Freundlich isotherm plot for adsorption of congo red onto layered double hydroxide**

The plot of  $\ln q_e$  against  $\varepsilon^2$  is shown in Fig. 8 and the constants  $q_D$  and  $B_D$  were calculated from the intercept and slope, respectively. The DKR isotherm parameters are given in Table 1. This plot as indicated from the regression parameter  $R^2$  (0.9982) showed that this isotherm provides a very good fit to the experimental data. If the value of  $E$  lies between 8 and 16 kJ/mol the sorption process is a chemisorptions one, while values of below 8 kJ/mol indicates a physical adsorption process<sup>12,17</sup>. The value of the apparent energy of adsorption (0.6871 kJ/mol) obtained indicated physisorptions between the layered double hydroxide and congo red dye.

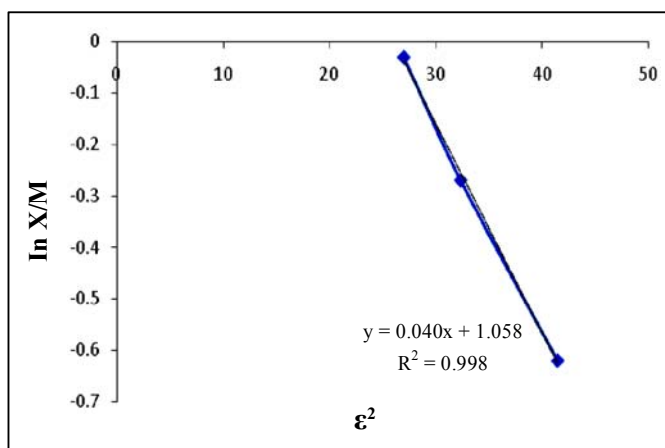


**Fig. 8: Dubinin-Kaganer-Radushkevich (DKR) isotherm plot for adsorption of congo red onto layered double hydroxide**

Temkin adsorption isotherm model is usually chosen to evaluate the adsorption potentials of an adsorbent for the adsorbate from an experimental data. This model gives the mechanism and adsorption capacity of an adsorbate in a sorption process.

This isotherm was applied by a linear plot of  $q_e$  against  $\ln C_e$  shown in Fig. 9 and the constants B and A were calculated from the slope and intercept, respectively. The Temkins isotherm parameters A, B and  $R^2$  are presented in Table 1. Again, looking at the regression  $R^2$  obtained (0.9992). It is seen that this isotherm is applicable to the description of equilibrium data.

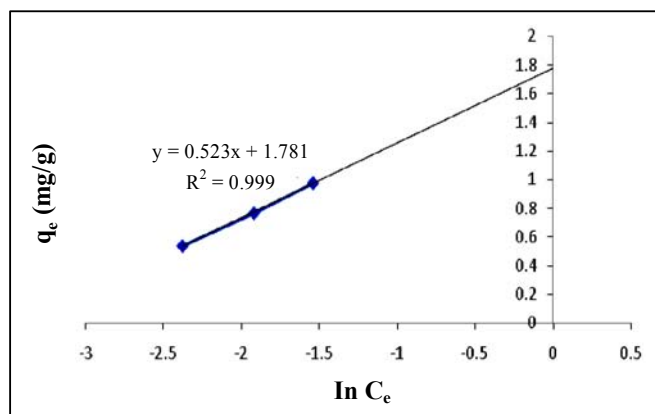


**Fig. 9: Temkin isotherm model plot for adsorption of congo red onto layered double hydroxide**

**Table 1: Characteristic parameters of the adsorption isotherm models for congo red adsorption by layered double hydroxide**

Isotherm model	Isotherm parameter	Results
Freundlich	$1/n$	1.0646
	$R^2$	0.9973
Langmuir	$K_L$ (mg/L)	0.714
	$R^2$	0.9995
	E (KJ/mol)	0.6871
Dubinin-Kaganer-Radushkevich	$\beta_D$ (mol <sup>2</sup> /KJ <sup>2</sup> )	1.0589
	$q_D$ (mg/g)	0.9602
	$R^2$	0.9982

Cont...

Isotherm model	Isotherm parameter	Results
Temkin	A	1.3412
	b	$1.27 \times 10^3$
	B	1.7814
	$R^2$	0.9992

### Effect of temperature

As shown in Fig. 10, adsorption was lowest at 313 K (53.5%), and increased slightly to 333 K (55%) and 353 K (58%). This means that adsorption capacity increase with higher temperature.

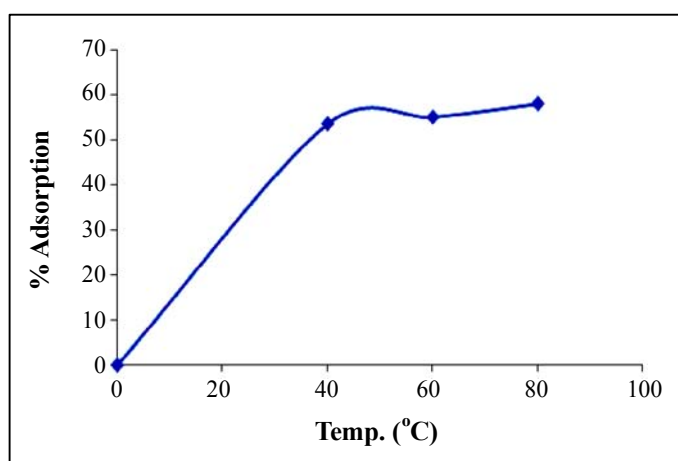


**Fig. 10: Effect of temperature on adsorption of congo red onto layered double hydroxide**

The values of the enthalpy change ( $\Delta H^0$ ) and entropy change  $\Delta S^0$  were calculated from equation 10 to be 4.2328 KJ/mol and 14.6 J/molK, respectively, as shown in Fig. 11. A positive  $\Delta H^0$  suggests that sorption proceeded favourably at a higher temperature and the sorption mechanism was exothermic. A positive value of  $\Delta S^0$  (14.6 J/molK) reflects the affinity of the adsorbent towards the adsorbate species. In addition, positive value of  $\Delta S^0$  suggests increased randomness at the solid/solution interface with some structural changes in the adsorbate and the adsorbent. The adsorbed solvent molecules, which are displaced by the adsorbate species, gain more translational entropy than is lost by the adsorbate ions/molecules, thus allowing for the prevalence of randomness in the system<sup>18</sup>. The positive  $\Delta S^0$  value also corresponds to an increase in the degree of freedom of the adsorbed species.

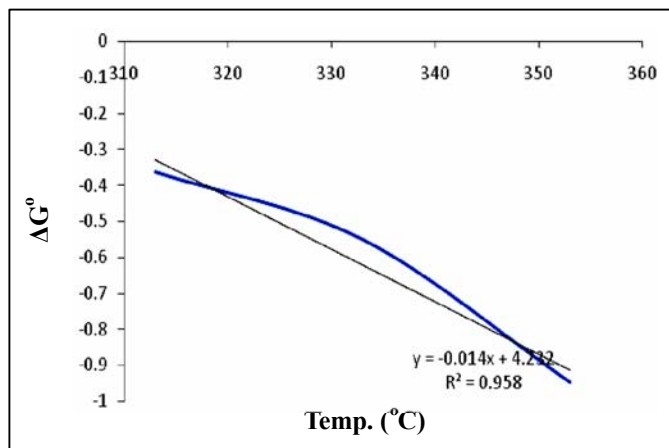


**Fig. 11: Plot of  $\Delta G^\circ$  vs. temperature for the adsorption of congo red onto layered double hydroxide**

Isosteric heat of adsorption  $\Delta H_x$  is one of the basic requirements for the characterization and optimization of an adsorption process and is a critical design variable in estimating the performance of an adsorptive separation process. It also gives some indication about the surface energetic heterogeneity. Knowledge of the heats of sorption is very important for equipment and process design. A plot of  $\ln C_e$  against  $1/T$  in Fig. 12 gives a slope equal to  $\Delta H_x$ . The value of  $\Delta H_x$  derived from equation 11 was 74.16 KJ/mol, which indicates that adsorption mechanism was chemical adsorption and in an heterogeneous surface<sup>18,19</sup>.

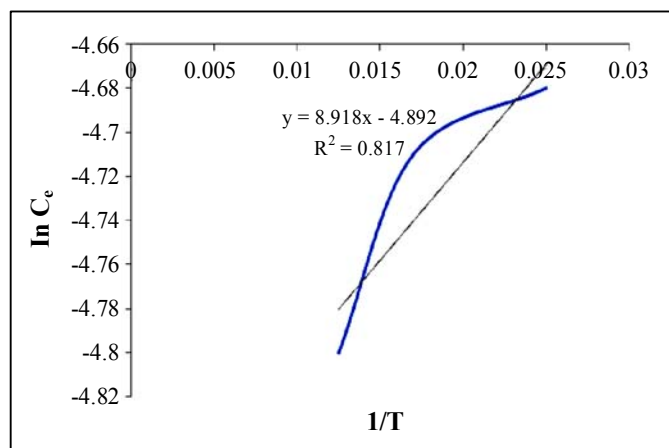


**Fig. 12: Plot of  $\ln C_e$  vs.  $1/T$  for the adsorption of congo red onto layered double hydroxide**

The activation energy  $E_a$  and the sticking probability  $S^*$  were calculated from equation 12, the value shown in table 1 for  $E_a$  and  $S^*$  are -11.77 KJ/mol and 0.47, respectively, as shown in the plot in Fig. 13. The value of activation energy shows that the sorption process was a physical one less than 4.2 KJ/mol<sup>12,19</sup>. The sticking probability  $S^*$  indicates the measure of the potential of an adsorbate to remain on the adsorbent. It is often interpreted as  $S^* > 1$  (no sorption),  $S^* = 1$  (mixture of physic-sorption and chemisorption),  $S^* = 0$  (indefinite sticking – chemisorption),  $0 < S^* < 1$  (favourable sticking-physic-sorption).

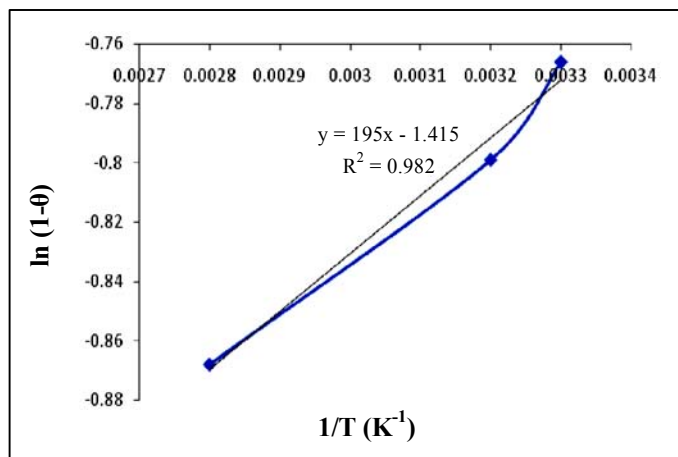


**Fig. 13: Plot of  $\ln(1-\theta)$  vs.  $1/T(K^{-1})$  for the adsorption of congo red onto layered double hydroxide**

**Table : Thermodynamic parameters of the adsorption of congo red onto layered double hydroxide**

T (K)	$\Delta G^{\circ}$ (KJ/mol)	$\Delta H^{\circ}$ (KJ/mol)	$\Delta S^{\circ}$ (J/molK)	$E_a$ (KJ/mol)	$\Delta H_x$ (J/molK)
313	-0.364				
333	-0.551	4.2328	14.6	-11.77	74.16
353	-0.947				

### Kinetic study

#### Effect of time

The adsorption kinetic study is important in predicting the mechanisms (chemical reaction or mass-transport process) that control the rate of the pollutant removal and

retention time of adsorbed species at the solid-liquid interface<sup>11,12</sup>. That information is important in the design of appropriate sorption treatment plants.

The effect of contact time of the phases on removal of congo red by the layered double hydroxide from solutions of initial concentration equal to 400 mg CR/L at three different times (10, 20 and 30 mins) is presented in Fig. 14.

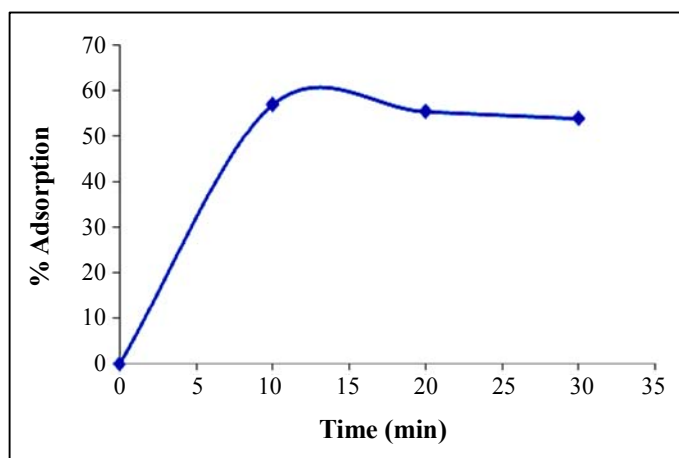


**Fig. 14: Effect of contact time on adsorption of congo red onto layered double hydroxide**

The result shows that adsorption was highest at 10 mins, thereafter, a gradual decrease occurred (10 = 57%, 20 = 55.5% and 30 = 54%).

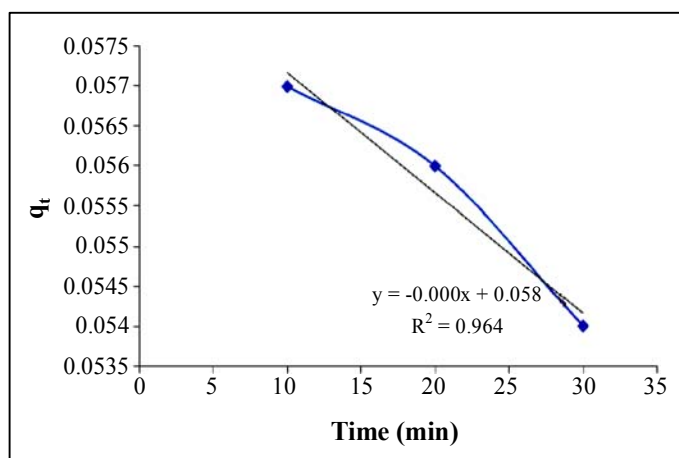


**Fig. 15: Plot of  $q_t$  vs.  $t$  for the adsorption of congo red onto layered double hydroxide**

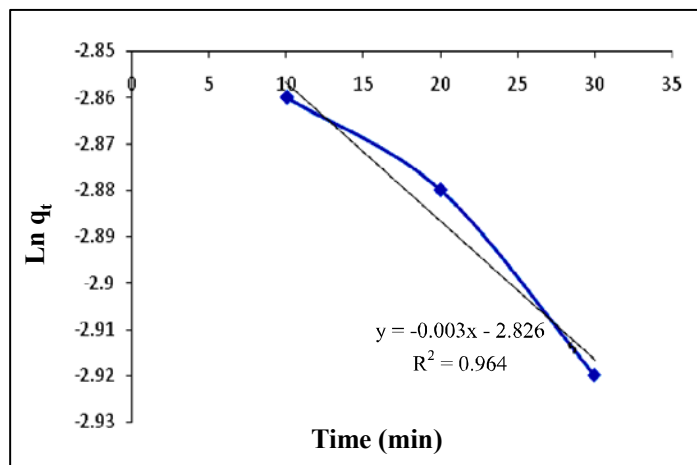


**Fig. 16:** Plot of  $q_t$  vs.  $t$  for the adsorption of congo red onto layered double hydroxide

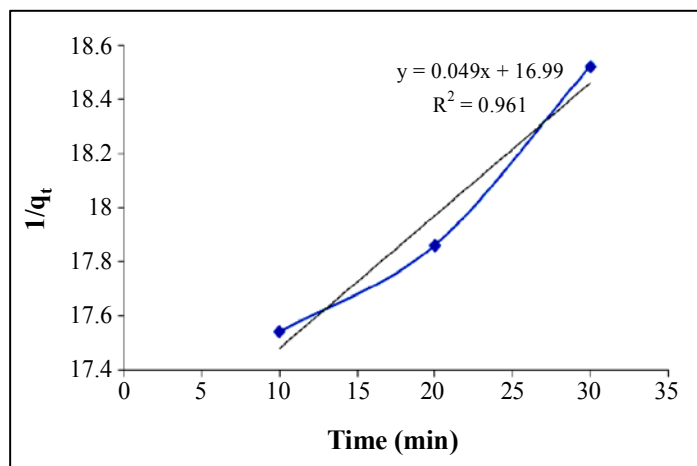


**Fig. 17:** Plot of  $1/q_t$  vs.  $t$  for the adsorption of congo red onto layered double hydroxide

The experimental data were fitted into different kinetic models including (Figs. 15-19) zero-order-kinetic model, first-order-kinetic model, second-order-kinetic model, pseudo-second-order-kinetic model and third-order-kinetic model to ascertain the suitability of the models. The correlation coefficient values of 0.9643, 0.9643, 0.9614, 0.9994 and 0.8929, respectively confirms the applicability of the above models with pseudo-second-order model been the best fit  $R^2 = 0.9994$ .

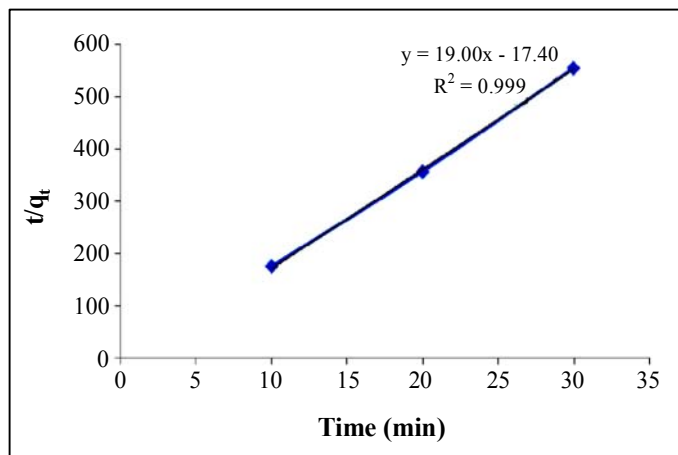


**Fig. 18: Plot of  $t/q_t$  vs.  $t$  for the adsorption of congo red onto layered double hydroxide**

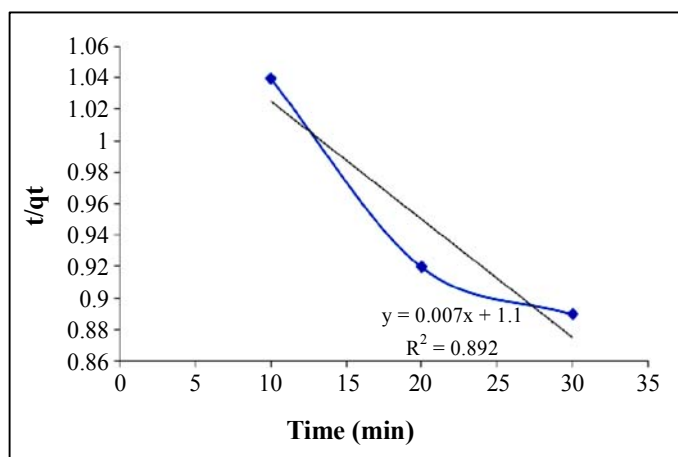


**Fig. 19: Plot of  $t/q_t$  vs.  $t$  for the adsorption of congo red onto layered double hydroxide**

## CONCLUSION

In the present work, it was found that adsorption of congo red using Ni/Fe-CO<sub>3</sub> is explained well by all isotherm models studied in this paper. The kinetic properties of the adsorption process was better defined by pseudo-second-order kinetic model. The thermodynamic parameters such as  $\Delta H^\circ$ ,  $\Delta S^\circ$  and  $\Delta H_x$  indicated that the adsorption process was endothermic and process is dependent on increase in temperature, thereby increasing the randomness of the solid/liquid phase of the reaction system. Therefore, to optimize the adsorption process, variation of operational parameters such as temperature and increasing

the amount of layered double hydroxide will no doubt further increase the adsorption of the congo red. The results overall indicated that layered double hydroxide could be considered a promising adsorbent for the removal of dyes from aqueous solutions.

## REFERENCES

1. H. Marsh and F. Rodríguez-Reinoso, *Activated Carbon*, Elsevier, Amsterdam (2006).
2. B. Noroozi, G. A. Sorial, H. Bahrami and M. Arami, Equilibrium and Kinetic Adsorption Study of a Cationic Dye by a Natural Adsorbent-Silkworm Pupa, *J. Haz. Mater.*, **B139**, 167-174 (2007).
3. A. Reife, Dyes, Environmental Chemistry, In Kirk-Othmer (Ed.), *Encyclopedia of Chemical Technology*, Washington: John Wiley & Sons (1993) p. 753.
4. U. Pagga and D. Braun, The Degradation of Dye Stuffs: Part II, Behaviour of Dyestuffs in Aerobic Biodegradation Tests, *Chemosphere*, **154**, 79-489 (1986).
5. J. R. Deans and B. G. Dixon, Uptake of  $Pb^{2+}$  and  $Cu^{2+}$  by Novel Biopolymers, *Water Res.*, **26(4)**, 469-472 (1992).
6. P. Nigam, G. Armour, I. M. Banat, D. Singh and R. Marchant, Physical Removal of Textile Dyes from Effluents and Solid-state Fermentation of Dye-adsorbed Agricultural Residues, *Bioresource Technol.*, **72**, 219-226 (2000).
7. F. Cavani, F. Trifiro and A. Vaccari, Hydrotalcite-type Anionic Clays: Preparation, Properties and Applications, *Catal Today*, **11**, 173-301 (1991).
8. F. N. Arslanoglu, F. Kar and N. Arslan, Adsorption of Dark Compounds from Peach Pulp by using Powdered Activation Carbon, *J. Food Eng.*, **71**, 156-163 (2005).
9. Y. Yasin, A. H. Abdul Malik, S. M. Sumari and B. H. A. Faujan, Removal of Amido Black Dye from Aqueous Solution by Uncalcined and Calcined Hydrotalcite, *R. J. Chem. Environ.*, **14(1)**, 78-84 (2010).
10. Y. Yasin, M. Mohamad and F. B. H. Ahmad, The Application of Response Surface Methodology for Lead Ion Removal from Aqueous Solution using Intercalated Tartrated-Mg-Al Layered Double Hydroxides, *Int. J. Chem. Eng.*, **2013**, 1-7 (2013).
11. N. Ayawei, A. T. Ekubo, D. Wankasi and E. D. Dikio, Synthesis and Application of Layered Double Hydroxide for the Removal of Copper in Wastewater, *Int. J. Chem.*, **7(1)**, 122-132 (2015).

12. N. Ayawei, A. T. Ekubo, D. Wankasi and E. D. Dikio, Equilibrium, Thermodynamic and Kinetic Studies of the Adsorption of Lead(II) on Ni/Fe Layered Double Hydroxide, *Asian J. Appl. Sci.*, **03(02)**, 207-217 (2015).
13. R. Gong, Y. Sun, J. Chen, H. Liu and C. Yang, Effect of Chemical Modification on Dye Adsorption Capacity of Peanut Hull, *Dyes and Pigments*, **67**, 175-181 (2005).
14. F. A. Dawodu, G. K. Akpomie and I. C. Ogbu, Isotherm Modeling on the Equilibrium Sorption of Cadmium (II) from Solution by Agbani Clay, *Int. J. Multidisciplinary Sci. Engg.*, **3(9)**, 9-14 (2012).
15. K. K. H. Choy, G. Mckay and J. F. Porter, Sorption of Acidic Dyes from Effluents using Activated Carbons, *Resource Conserv. Recycling*, **27**, 57-71 (1999).
16. P. Sivakumar and P. N. Palanisamy, Adsorption Studies of Basic Red 29 by a Non Conventional Activated Carbon Prepared from Euphorbia Antiquorum L, *Int. J. Chem. Tech. Res*, **1(3)**, 502-510 (2009).
17. G. Ahmet, Synthesis and Characterization of Hybrid Congo Red from Chloro-Functionalized Silsesquioxanes, *Turk J. Chem.*, **34**, 437-445 (2009).
18. N. Ayawei, A. T. Ekubo, D. Wankasi and E. D. Dikio, Synthesis and Application of Layered Double Hydroxide for the removal of Copper in Wastewater, *Int. J. Chem.*, **7(1)**, 122-132 (2015).
19. N. Ayawei, A. T. Ekubo, D. Wankasi and E. D. Dikio, Adsorption Dynamics of Copper Adsorption by Zn/Al-CO<sub>3</sub>, *Int. J. Adv. Chem. Sci. App.*, **3(1)**, 57-64 (2015).

*Revised : 17.05.2015*

*Accepted : 19.05.2015*